Inorganic Chemistry
Article
pubs.acs.org/IC

Magnetic and Photochromic Properties of a Manganese(II) Metal-Zwitterionic Coordination Polymer

Teng Gong, Xiao Yang, Qi Sui, Yan Qi, Fu-Gui Xi, and En-Qing Gao*

Shanghai Key Laboratory of Green Chemistry and Chemical Processes, College of Chemistry and Molecular Engineering, East China Normal University, Shanghai 200062, China

Ⓢ *Supporting Information*

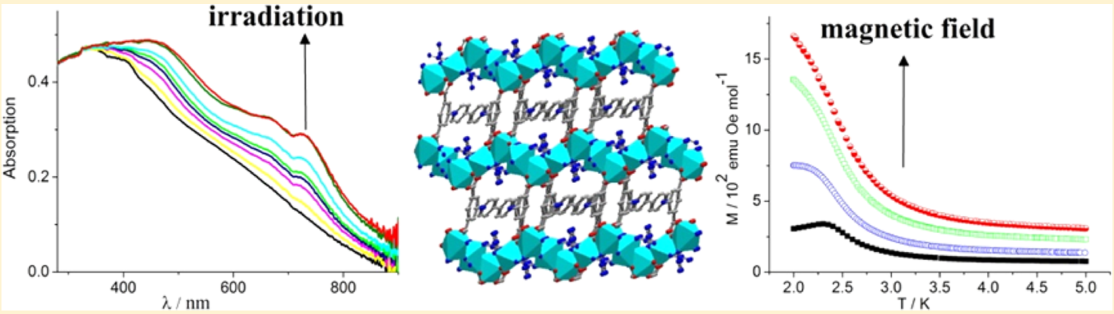

ABSTRACT: The solvothermal reaction of $Mn(ClO_4)_2$, NaN_3, and a rigid viologen-tethered tetracarboxylic acid (1,1′-bis(3,5-dicarboxyphenyl)-4,4′-bipyridinium chloride, $[H_4L]Cl_2$) led to a coordination polymer of formula $[Mn_4(L)(N_3)_6(H_2O)_2]_n$. X-ray analysis revealed a 3D coordination structure. The Mn(II) ions are connected by mixed azide and carboxylate bridges to give 2D layers, which are pillared by the viologen tether of the zwitterionic ligand. Magnetic analyses suggested that the compound features antiferromagnetism and field-induced metamagnetism. The compound also shows photochromic and photomagnetic properties. The long-range magnetic ordering is owed to the spin-canting structure of the Mn(II)-azide-carboxylate layer; the photochromism involves the formation of viologen radicals via photoinduced electron transfer, and the photomagnetism is related to the interactions between the metal ion and the photogenerated radicals. The study demonstrates a strategy for the design of new multifunctional materials with photoresponsive properties.

■ INTRODUCTION

Multifunctional molecular materials have caught much attention for decades, because of their potential applications in information storage,[1] molecular switches,[2] sensing,[3] energy conversion,[4] etc.[5] Coordination polymers or metal−organic frameworks, which can combine functional organic linkers and metal ions, provide versatile platforms for designing multifunctional materials.[6] In this context, the coordination systems containing both photosensitive and magnetic components have been of great interest. Among others, photomagnetic coordination compounds with photoinduced spin-crossover,[7] valence tautomerism,[8] or intermetallic charge transfer have been extensively studied.[9]

Viologen cations (V^{2+}, *N,N′*-disubstituted 4,4′-bipyridiniums) are electron-deficient species exhibiting excellent charge-transfer and redox properties with photoactivity.[10] The availability of three oxidation states (V^{2+}, $V^{\bullet+}$, and V^0) has evoked much interest in the study of viologens as catalysts or electron relays in chemical or photochemical redox systems and as chemo-/electro-/photoresponsive materials for applications such as electrochromic display,[11] smart windows,[12] molecular machines,[13] and switches.[14] The propensity of viologens to form charge-transfer complexes with electron-rich species has allowed for their wide use as active components in supramolecular assemblies for molecular recognition inclusion and sensing.[15] Recently, some zwitterionic viologen derivatives bearing carboxylate as coordinative group have been used to construct coordination polymers, most of which contain diamagnetic metal ions. Selective guest adsorption,[16] photochromism,[17] photomodulated luminescence,[18] or mechanochromic luminescence[19] has been demonstrated for some of these "metal-viologen" coordination polymers.[20] With interest in molecular magnetism, we have recently utilized pyridinium-based zwitterionic carboxylate ligands in combination with azide to develop new superexchange pathways and new magnetic materials. The approach has led to some azide-carboxylate mixed-bridge systems that are not or rarely accessible from nonzwitterionic carboxylate ligands. Various magnetic properties, such as ferromagnetic coupling, single-chain magnetism, and solvent-modulated magnetism, have been observed in the mixed-bridge systems.[21]

Considering the respective success in photochromic and magnetic studies on coordination polymers with viologen-carboxylate zwitterions, we initiated a project to search new multifunctional systems exhibiting both photochromic and

Received: August 17, 2015

DOI: 10.1021/acs.inorgchem.5b01888
Inorg. Chem. XXXX, XXX, XXX−XXX

(photo)magnetic properties. A three-in-one synthetic strategy has been applied, with viologen groups as photoresponsive components, paramagnetic metal ions as spin carriers, and azide and carboxylate as mixed pathways for extended superexchange. In this Article, we report a Mn(II) coordination polymer of formula $[Mn_4(L)(N_3)_6(H_2O)_2]_n$ (**1**), which is derived from the rigid viologen-based tetracarboxylic ligand 1,1′-bis(3,5-dicarboxyphenyl)-4,4′-bipyridinium dichloride ($[H_4L]Cl_2$, Chart 1).

Chart 1. $[H_4L]Cl_2$ Ligand

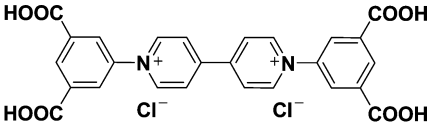

Some flexible viologen-based di- and tetracarboxylic ligands, with CH_2 groups between viologen and carboxylate groups, have been used to synthesize coordination compounds, but the coordination chemistry of the rigid analogues remained unexplored prior to this study. In **1**, complex 2D magnetic layers with mixed azide and carboxylate bridges are interlinked by the rigid backbone of the ligand. The compound shows the coexistence of spin-canted antiferromagnetism, metamagnetism, photochromism, and photomagnetism.

EXPERIMENTAL SECTION

Physical Measurements. NMR spectra were recorded on a Bruker Advance 400 MHz spectrometer. FT-IR spectra were recorded in the range 500−4000 cm^{-1} using KBr pellets on a Nicolet NEXUS 670 spectrophotometer. Elemental analyses were determined on an Elementar Vario ELIII analyzer. Powder X-ray diffraction (PXRD) was recorded on a Rigaku Ultima IV X-ray diffractometer equipped with a Cu-target tube at 35 kV, 25 mA, and a graphite monochromator. UV−vis spectra were determined on a SHIMADZU UV-2700 spectrometer. $BaSO_4$ plates were used as references (100% reflection), on which the finely ground power of a sample was coated. Electron spin resonance (ESR) spectra were recorded on a Bruker Elexsys 580 spectrometer with a 100 kHz magnetic field in the X band at room temperature. X-ray photoelectron spectroscopy (XPS) studies were performed with a PHI 5000 Versaprobe spectrometer using Al Kα radiation (λ = 8.357 Å). Temperature-dependent and field-dependent magnetic measurements were carried out on a Quantum Design SQUID MPMS-5 magnetometer. Diamagnetic corrections were made with Pascal's constants. A CEL-HXUV300 300W xenon lamp system equipped with an IR filter was used for photochromic studies, and the distance between the sample and the Xe lamp was around 40 cm.

Synthesis. All the reagents and solvents employed were commercially available and used without further purification. *N,N*′-Bis(2,4-dinitrophenyl)-4,4′-bipyridinium dichloride was prepared according to literature procedures.[22]

Caution! *Although not encountered in our experiments, azide compounds of metal ions are potentially explosive. Only a small amount of the materials should be prepared, and it should be handled with care.*

Synthesis of $[H_4L]Cl_2$. To *N,N*′-bis(2,4-dinitrophenyl)-4,4′-bipyridinium dichloride (0.99 g, 1.86 mmol) dissolved in 50% EtOH (60 mL) was added dimethyl-5-aminoisophthalate (1.69 g, 8.1 mmol), and the mixture was stirred for 36 h at 90 °C. The solvent was evaporated, and the residue dissolved in H_2O. After filtering off the insolvable solid, the filtrate was washed with Et_2O three times and evaporated to give a crude product of 1,1′-bis(3,5-bis(methoxycarbonyl)phenyl)-4,4′-bipyridinium dichloride ($[Me_4L]Cl_2$). The products were recrystallized from methanol/ethyl acetate to give yellow powder. Yield: 0.58 g (50.9%). ^1H NMR (400 MHz, D_2O): δ = 9.48 (d, *J* = 6.4 Hz, 4H), 8.95 (s, 2H), 8.86 (d, *J* = 6.4 Hz, 4H), 8.68 (s, 4H), 4.00 (s, 12H). $[Me_4L]Cl_2$ (0.58g, 0.95 mmol) dissolved in concentrated HCl (8 mL) was refluxed for 24 h. The solid product was filtrated, washed with water and acetone, and dried under vacuum. $[H_4L]Cl_2$ was obtained as pale yellow powder. Yield: 0.48 g (90.6%). ^1H NMR (400 MHz, DMSO-d_6): δ = 9.80 (d, *J* = 6.9 Hz, 4H), 9.13 (d, *J* = 6.9 Hz, 4H), 8.76 (t, *J* = 1.3 Hz, 2H), 8.72 (d, *J* = 1.3 Hz, 4H). Anal. Calcd for $C_{26}H_{18}N_2O_8Cl_2$ (*M* = 557.34): C, 56.03; H, 3.26; N, 5.03; Cl, 12.72. Found: C, 55.85; H, 3.16; N, 5.28; Cl, 12.66%.

Synthesis of $[Mn_4(L)(N_3)_6(H_2O)_2]_n$ (1). NaN_3 (0.112 g, 1.72 mmol) and $Mn(ClO_4)_2$ $6H_2O$ (0.033 g, 0.090 mmol) were mixed in H_2O/CH_3OH (3:1 v/v 4 mL) and stirred for 10 min. Then, $[H_4L]Cl_2$ (0.005 g, 0.009 mmol) was added with stirring. The resulting suspension was kept at 100 °C for 18 h in a sealed glass bottle. The brown crystals were rinsed by H_2O several times, separated by filtration, and dried in air. Yield: 54%. The phase purity of the bulk product was confirmed by PXRD experiments (Figure S1, Supporting Information). Anal. Calcd for $C_{26}H_{18}N_{20}O_{10}Mn_4$ (*M* = 990.30): C, 31.53; H, 1.83; N, 28.29. Found: C, 31.35; H, 1.74; N, 28.17%. Main IR (KBr, cm^{-1}): 3443br, 3083m, 3039m, 2125s, 2062vs, 1635m, 1618m, 1607m, 1562s, 1458m, 1433m, 1385s (Figure S2, Supporting Information).

X-ray Crystallography. Diffraction intensity data of **1** were collected at 296 K on a Bruker APEX II diffractometer equipped with a CCD area detector and graphite-monochromated Mo Kα radiation (λ = 0.710 73 Å). The compound was determined to be a nonmerohedral twin composed of two crystal domains. A twin law was created, and the data was corrected for Lorentz and polarization effects and absorption using TWINABS.[23] The structure was solved by direct methods and refined by the full-matrix least-squares method on F^2, with all non-hydrogen atoms refined with anisotropic displacement parameters.[24] All hydrogen atoms attached to carbons were calculated geometrically and refined using the riding model. Water hydrogen atoms were located from the difference map and refined isotropically. A summary of the crystallographic data, data collection, and refinement parameters is provided in Table 1.

Table 1. Crystallographic Data and Structure Refinements Parameters for Compound 1

empirical formula	$C_{26}H_{18}N_{20}O_{10}Mn_4$
fw	990.36
cryst syst	triclinic
space group	$P\overline{1}$
a, Å	8.037(3)
b, Å	10.192(3)
c, Å	11.154(4)
α, deg	104.877(5)
β, deg	98.307(5)
γ, deg	103.873(5)
V, Å^3	836.4(5)
Z	1
ρ_{calcd}, g cm^{-3}	1.966
μ, mm^{-1}	1.567
θ range collected	2.16−26.26
S on F^2	1.125
R1, wR2 [$I > 2\sigma(I)$]	0.0374, 0.1523
R1, wR2 (all data)	0.0439, 0.1847

RESULTS AND DISCUSSION

Synthesis. Our synthetic approach toward the targeted ligand followed a general procedure for similar symmetric diaryl viologens (Scheme 1). In the key step, the Zincke reaction[25] of *N,N*′-bis(2,4-dinitrophenyl)-4,4′-bipyridinium dichloride with dimethyl 5-aminoisophthalate gave $[Me_4L]Cl_2$ in medium yield, which was hydrolyzed in concentrated HCl solution to afford $[H_4L]Cl_2$. The organic salt is insoluble in common solvents

Scheme 1. Synthesis of the $[H_4L]Cl_2$ Ligand

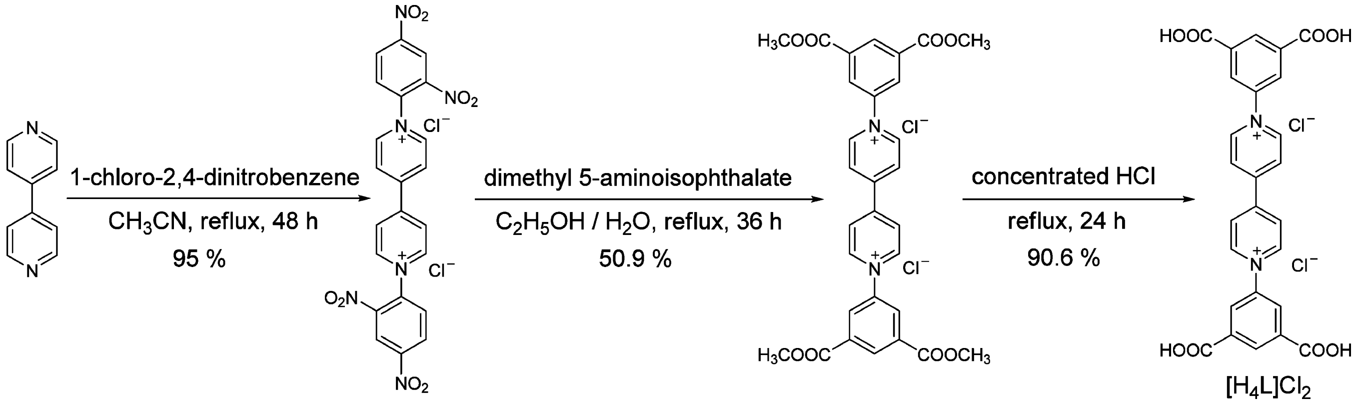

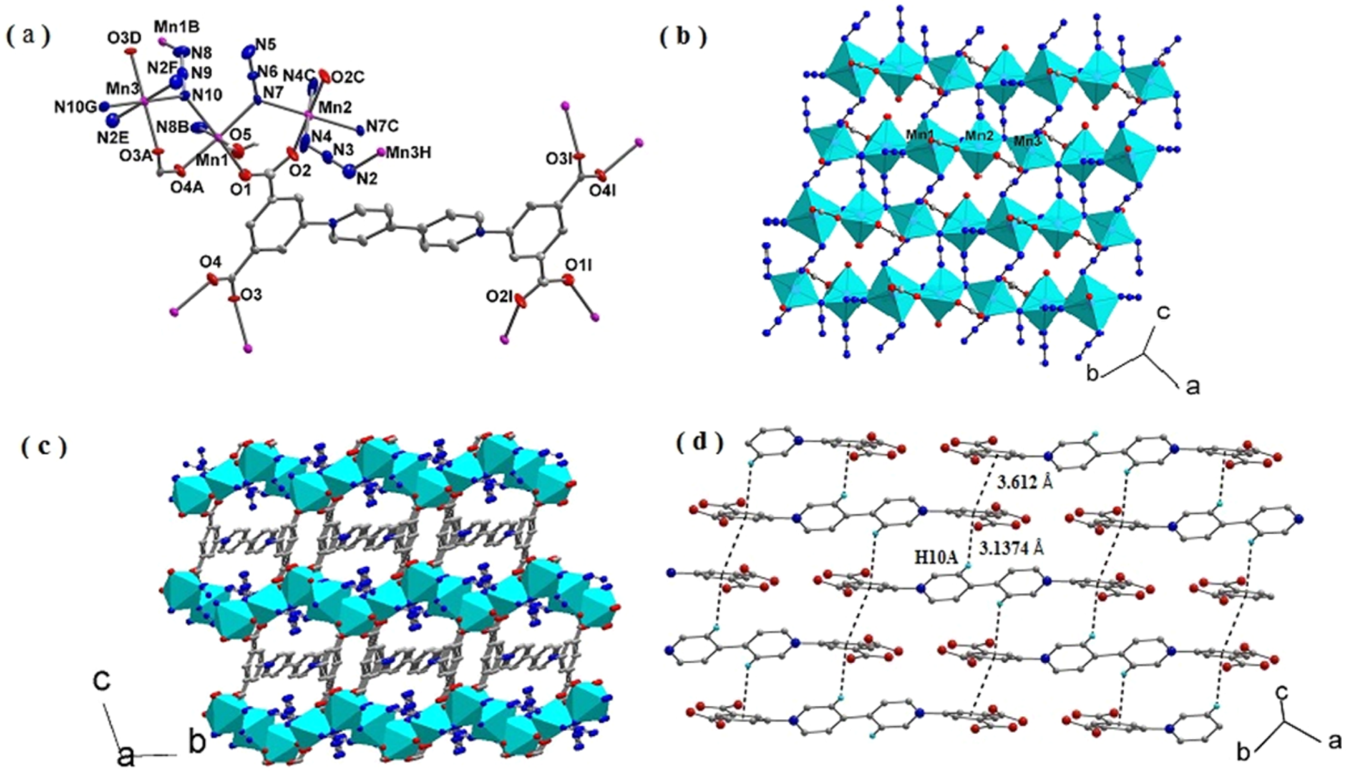

Figure 1. Structure of **1**. (a) Coordination environments of the metal ion and the ligands. Symmetry code: A = −*x* + 2, −*y*, −*z*; B = −*x* + 2, −*y*, −*z* + 1; C = −*x* + 2, −*y* + 1, −*z* + 1; D = *x* + 1, *y*, *z* + 1; E = *x*, *y* − 1, *z*; F = −*x* + 3, −*y* + 1, −*z* + 1; G = −*x* + 3, −*y*, −*z* + 1; H = *x*, *y* + 1, *z*; I = −*x*, −*y* + 1, −*z*. (b) Top view of the 2D layer. (c) The 3D structure, and (d) $\pi\cdots\pi$ and C−H$\cdots\pi$ interactions among the ligands.

including water, alcohols, and DMF, but soluble in water in the presence of bases. Complex **1** was solvothermally synthesized from $Mn(ClO_4)_2$, NaN_3, and $[H_4L]Cl_2$ in aqueous methanol. NaN_3 serves as a weak base to deprotonate the ligand and also as anionic ligand to coordinate with metal ions. It proved that a large excess of NaN_3 was necessary to obtain complex **1** as pure phase.

Crystal Structures. Single-crystal X-ray structure analysis revealed that compound **1** crystallizes in the triclinic space group $P\bar{1}$ and exhibits a 3D coordination network (Figure 1). There are three independent Mn(II) sites. Mn1 is ligated by three azide nitrogens, two carboxylate oxygens, and a water molecule in a $[N_3O_3]$ *fac*-octahedral geometry. Mn2 and Mn3 reside in centrosymmertric $[N_4O_2]$ *trans*-octahedral environments completed by four azide nitrogens and two carboxylate oxygens. The Mn−O and Mn−N distances lie in the ranges 2.105(4)−2.158(3) and 2.193(4)−2.312(4) Å, respectively. The azide ions adopt three different coordination modes. The N5−N6−N7 azide serves as μ-1,1 bridge between Mn1 and Mn2 with Mn−N7−Mn = 118.9(2)°, N2−N3−N4 as μ-1,3 bridge between Mn2 and Mn3H with an Mn−N_3−Mn torsion angle of 100.9(3)°, and N8−N9−N10 as μ-1,1,3 bridge among Mn1, Mn3, and Mn1B, with Mn1−N10−Mn3 = 122.5(2)°. The μ-1,1 or μ-1,1,3-azide bridges collaborate with μ-1,3-caboxylate bridges from the L ligand to connect the metal ions in the Mn1−Mn2−Mn1−Mn3 sequence along the (1−10) direction, giving rise to a chain with (μ-1,3-COO)(μ-1,1-N3) double bridges. Adjacent $[MnN_3O_3]$ and $[MnN_4O_2]$ octahedrons along the chain share corners (the bridging N7 and N10 atoms) and are slanted with respect to each other owing to the angular Mn−N−Mn linkage. The Mn1$\cdots$Mn2 and Mn1$\cdots$Mn3 distances spanned by the double bridges are 3.863(1) and

3.927(1) Å, respectively. The chains are further linked into a 2D layer through μ-1,3 and μ-1,1,3-azide bridges (Figure 1b). The μ-1,3 bridge defines an interchain Mn⋯Mn distance of 5.683(1) Å, and the interchain distances defined by the 1,3 motif of the μ-1,1,3 bridge are 5.655(2) and 5.497(2) Å.

The fully deprotonated L ligand lies at an inversion center, and the two pyridinium rings are coplanar. The neighboring benzene and pyridinium rings have a dihedral angle of 30.5(1)°. The ligand binds eight metal ions with each carboxylate groups acting as μ-1,3 bridges. The two carboxylate groups from each *m*-benzenedicarboxylate moiety bind two different layers, and thus, the formally anionic $[Mn_2(N_3)_3(COO)_2]$ layers are charge compensated and linked by the cationic bipyridinium backbone of the ligand to generate a 3D framework (Figure 1c). The ligands extend in parallel to the layers, so the interlayer distance (10.52 Å) is determined by the *m*-benzenedicarboxylate moiety. The interlayer Mn⋯Mn distances spanned by the moiety are 7.801(3)−10.704(4) Å. In addition, the interlayer ligands are arranged in an offset fashion and associated into a 2D array *via* $\pi-\pi$ and H⋯π interactions (Figure 1d). Two benzene rings from two ligands related by an inversion center overlap in a face-to-face way, with an interplanar distance of 3.34 Å and a center-to-center distance of 3.612(1) Å. Furthermore, a pyridyl H atom (H10A) from one ligand is 3.033(1) Å above a benzene plane from another ligand, with an H⋯G distance of 3.317(1) Å (G is the center of the benzene ring involved).

Photochromism. $[H_4L]Cl_2$ and complex **1** both show color change upon illumination with Xe light (Figure 2). The pale yellow powder sample of $[H_4L]Cl_2$ turns to green after illumination for 1 min. The green photoproduct can be kept in air without color change for 3 days, but the color slowly changes back to pale yellow upon prolonged standing in air. The color recovery can be completed by annealing at 80 °C in air for 1 h. The color change can be repeated at least 5 times. The color change is different from dimethyl viologen, which turns from colorless to blue upon illumination.[26] This could be because the direct attachment of the rigid benzenedicarboxylic moieties to bipyridinium lowers the transition energy. UV−vis reflectance spectra were measured before and after illumination (Figure 2). The original sample shows strong and structured absorption bands below 370 nm, with rapidly decreased tailing in the visible light region. The absorption should be related to the $\pi-\pi^*$ and n$-\pi^*$ transitions of the conjugated L ligand. The photoproduct of the ligand displays four new bands centered at 445, 532, 665, and 733 nm, which tend to saturate after illumination for 10 min.

Compound **1** changes its color from brown to dark brown when illuminated by a 300 W Xe lamp. Compared with the ligand, the solid state UV−vis spectrum of the complex (Figure 2) exhibits maximum absorption in the region of 230−400 nm and extends far into the visible light region, which should be due to the contribution from the charge-transfer transitions between Mn(II) and the L/azide ligands (the d−d transitions of Mn(II) is spin forbidden). Irradiation of the complex with Xe light increases the absorption in the visible light region, which develops into new bands centered at 460, 665, and 730 nm upon prolonged irradiation. The new bands tend to saturate after irradiation for 15 min.

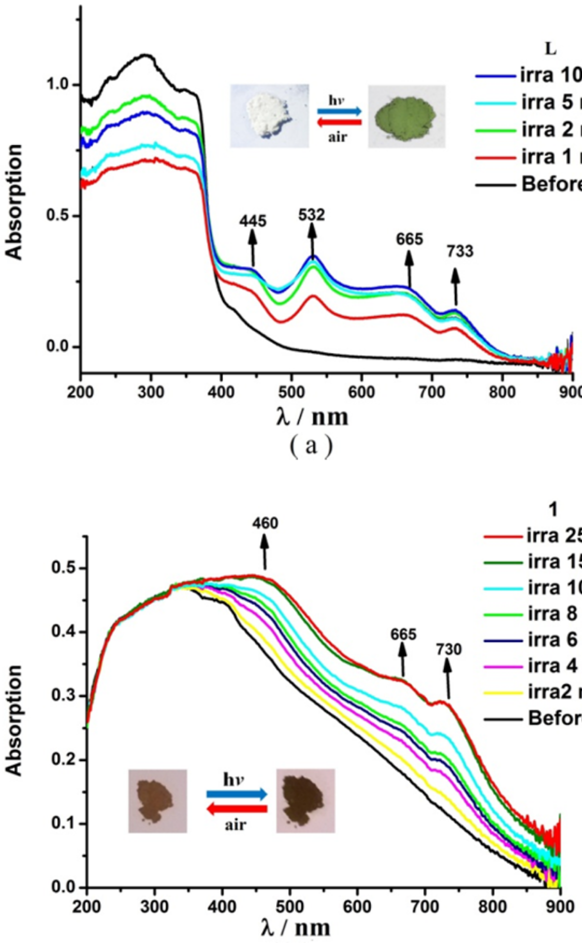

Figure 2. UV−vis diffuse reflectance spectra and photographs showing the photochromic behavior of $[H_4L]Cl_2$ and **1**.

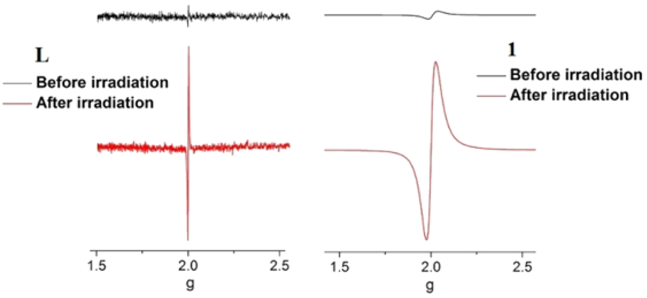

Figure 3. ESR spectra for $[H_4L]Cl_2$ and **1** before and after irradiation in the solid state at room temperature.

The photochromism of viologens is believed to be due to the generation of radicals ($V^{+\bullet}$) through photoinduced electron transfer. ESR measurements were performed to confirm the photogenerated radicals.[10b] After irradiation, $[H_4L]Cl_2$ exhibits a strong and sharp resonance signal with a *g* value of 2.0011 (Figure 3), close to that of a free electron (2.0023) and assignable to radicals.[27] The ligand salt shows a very weak signal at the same position before irradiation, which could be due to the presence of residual radicals. For complex **1** before irradiation, the signal observed at g = 2.0012 is significantly broader than expected for a radical and should be assigned to the Mn(II) ion, and it is uncertain whether the signal has a contribution from residual radicals. After irradiation, the signal of the complex is dramatically increased in intensity, confirming the formation of radicals.

DOI: 10.1021/acs.inorgchem.5b01888
Inorg. Chem. XXXX, XXX, XXX−XXX

The photoproduct of **1** returns to the original color more readily than the ligand. It can occur by standing overnight at room temperature or by annealing in air at 80 °C for 30 min. However, no significant color change was observed for the photoproducts of both $[H_4L]Cl_2$ and **1** in absence of air, even heated at 80 °C for 24 h. This could suggest that dioxygen plays an important role in quenching the photoinduced radical. The photochromic reversibility in air was confirmed by UV−vis and ESR measurements. The cyclical color change can be repeated for at least 5 times. The PXRD and IR data of the complex **1** (Figures S1 and S2) show no appreciable variation during the reversible process, suggesting that the crystal and molecular structure remains intact and excluding the possibility of photoinduced dissociation or rearrangement reactions.

XPS measurements were performed with complex **1** to probe the electron transfer process (Figure 4). The Mn 2p components show no appreciable change before and after Xe light irridation, indicating that Mn(II) ions are not involved in electron transfer. The maximum of the broad O 1s band prominently shifts to higher energy (from 531.06 to 531.23 eV) upon irradiation, suggesting that the photochromism should involve O atoms as electron donors. The N 1s spectra show two well-resolved bands at 398.6 and 402.6 eV. The low-energy band is attributable to the terminal N atoms of azide ions, while the high-energy one could have contributions from both the pyridinium N atoms and the central N atoms of azides.[28] The intensity ratio of the two bands (I_{403}/I_{399}) is 0.78, well-correlated with the ratio of the N atoms in the compound (3/4). The C 1s spectra are more complex, with three apparent bands at about 284.8, 286.0, and 288.1 eV, which are difficult to assign because of the presence of various C atoms in the compound. After irradiation, the binding energies of the N 1s and C 1s bands show no significant changes. However, there is an appreciable increase in the relative intensity of the C 1s band at the lowest binding energy, which could be due to the occurrence of electron transfer to pyridinium groups. The effect of the electron transfer on N bands may be obscured by the presence of azide N atoms, which predominate over pyridinium N atoms in amount.

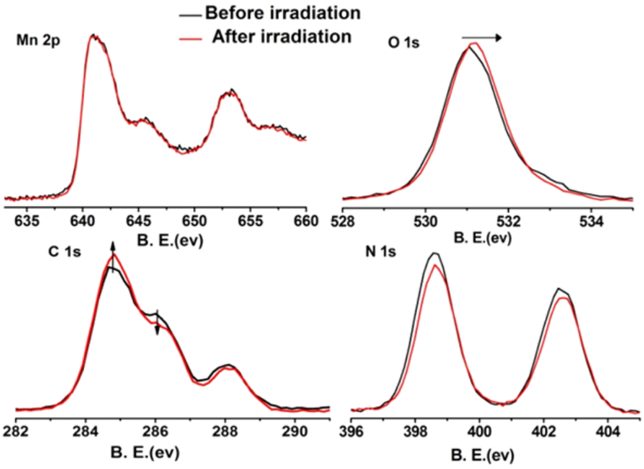

Figure 4. XPS core-level spectra of **1** before and after irradiation.

The electron transfer to viologens in the solid state has been related to the short contact between the pyridinium N atom and the donor[10b,d,16f] or weak hydrogen bonds between pyridinium C−H and the donor.[10c] In complex **1**, the shortest $N_{pyridinium}\cdots O$ distance is 3.918(6) Å, and the shortest $H_{pyridinium}\cdots O$ distance is 2.949(3) Å, where the O atoms arise from carboxylate groups. The distances are quite far for electron transfer. However, we noticed a short C−H···π contact between a pyridinium C−H group and the isophthalate group (Figure 1d), which may be a possible electron transfer pathway.

Magnetic and Photomagnetic Properties. The magnetic susceptibilities of **1** were measured in the 2−300 K temperature range under 1 kOe and are shown as χT versus T plots in Figure 5. The χT value at 300 K is 12.9 emu K mol^{-1}, significantly lower than the spin-only value (17.5 emu K mol^{-1}) for four magnetically isolated high-spin Mn(II) ions (S = $^5/_2$). The product first decreases smoothly to a minimum of 1.51 emu K mol^{-1} at 4 K, and then rises rapidly. The $1/\chi$ versus T data above 45 K follows the Curie−Weiss law with C = 14.7 emu mol^{-1} K and θ = −38.8 K. The behaviors above 4 K clearly indicate overall antiferromagnetic exchange. The structural data indicate that there are five different short superexchange pathways between neighboring Mn(II) ions in the azide- and carboxylate-bridged layer of **1** (Figures 1b and 6): three independent triatomic N−N−N pathways related to μ-1,3-N_3 (J_5) and μ_3-1,1,3-N_3 (J_3 and J_4), and two independent mixed-bridge (μ-1,3-COO)(μ-N) pathways, where the monatomic μ-N bridge arises from 1,1-N_3 (J_1) or μ_3-1,1,3-N_3 (J_2). The lack of

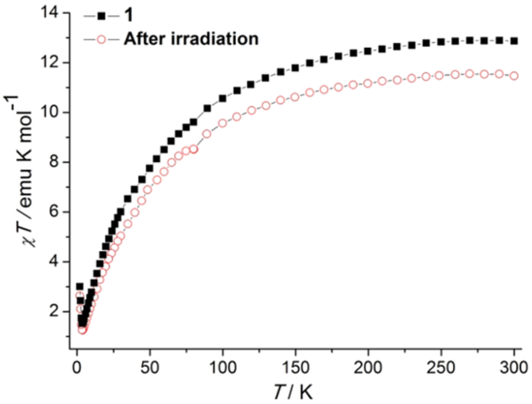

Figure 5. Temperature dependence of χT for **1** before and after irradiation at 1 kOe.

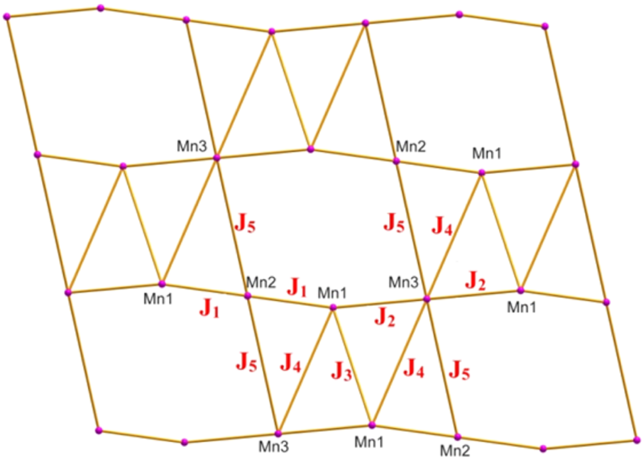

Figure 6. Spin coupling network in the layer of **1**. J_1–J_5 represent the independent superexchange pathways between neighboring Mn(II) ions (see text for corresponding bridging moieties).

appropriate models for the complicated coupling network precludes quantitative evaluation of the exchange parameters. However, the overall antiferromagnetic exchange can be qualitatively explained according to the bridging moieties between Mn(II) ions. It has been established that the N−N−N and μ-1,3-COO pathways are universally antiferromagnetic for Mn(II).[29] Although the μ-N bridge from 1,1-N_3 or μ_3-1,1,3-N_3 usually mediates ferromagnetic exchange between Mn(II) ions,[29b,31] previous studies have also demonstrated that the mixed μ-N and μ-1,3-COO bridges always induce antiferromagnetic interactions in Mn(II) compounds.[21d,e,30] Therefore, we can assume that all pathways in the layer of **1** mediate antiferromagnetic coupling.

The steep rises in the χT value of **1** at low temperature indicate the onset of a ferromagnetic-like correlation. This phenomenon is attributable to spin canting:[32] the antiferromagnetically coupled adjacent spins within the layer are not perfectly antiparallel but canted to each other, resulting in uncompensated moments for the layer. The occurrence of spin canting is consistent with the relatively slanted arrangement of metal polyhedrons throughout the layer.

To inspect into the low-temperature behaviors, variable-temperature magnetization was measured under different fields (Figure 7). The magnetization under low field (200 Oe) shows a maximum at about 2.3 K, indicating the onset of antiferromagnetic ordering due to weak antiferromagnetic interactions between spin-canted layers. The maximum disappears under high field (e.g., 400 Oe). This suggests a metamagnetic behavior: the antiferromagnetic interlayer interactions are overcome by high applied field, and an antiferro- to ferromagnetic state transition occurs.[33] The field-induced metamagnetism is confirmed by the sigmoid shape of the isothermal magnetization curve (Figure 8), from which the metamagnetic critical field is calculated to be 350 Oe (the field at which dM/dH shows maximum). The magnetization at high field increases rather slowly and quasilinearly, and the value (3.1 Nβ) at 50 kOe is far from the saturation value (20 Nβ) expected for four Mn(II) ions. These features are consistent with canted antiferromagnetism. Extrapolating the high-field linear part of the magnetization curve to zero field gives a value of 0.7 Nβ, and taking this as the contribution (M_w) of spin canting to the total magnetization, the canting angle can be estimated to be 2°.[34] Isothermal magnetization measurements with cycling field revealed a very narrow hysteresis loop with the double sigmoid shape typical of metamagnetism (Figure S3, Supporting Information).

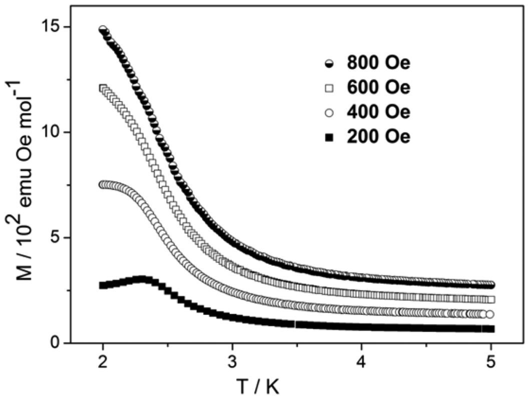

Figure 7. FC magnetization curves of **1** at 200, 400, 600, and 800 Oe.

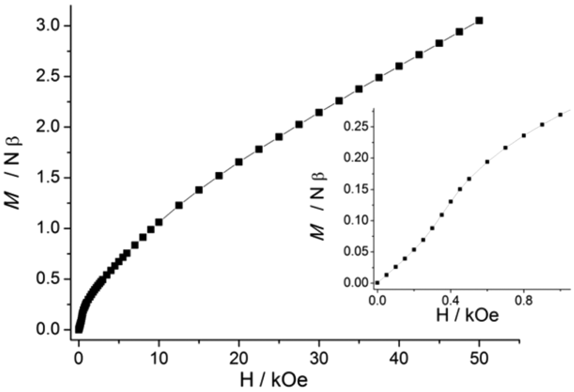

Figure 8. Isothermal magnetization curve of **1** at 2 K. The inset shows the low-field parts of the magnetization curves at 2 K.

To get insight into the photomagnetic properties, the variable-temperature magnetic properties of the complex were measured after Xe-lamp irradiation. The data are included in Figure 5. The variation of χT with temperature is similar to that before irradiation, but the χT values are reduced in the whole temperature range measured. The value at 300 K is 11.5 emu K mol^{-1}, lower by about 11% than the value before irradiation. The phenomenon was confirmed by repeated measurements using samples irradiated in air or in nitrogen atmosphere. Considering the formation of radicals upon irradiation, the reduction of magnetic susceptibility is rather unexpected. A possible interpretation is to assume that strong antiferromagnetic coupling is operative between Mn(II) and the photoinduced radical. The coupling should be strong enough to significantly reduce the magnetic moment even at room temperature. The mechanism is open to further investigation. The complicated spin coupling network in **1** makes it difficult to get exact information about the magnetic interactions.

■ CONCLUSIONS

A new bifunctional 3D coordination polymer has been synthesized from a viologen-based zwitterionic tetracarboxylate ligand. In the compound, μ-1,1-azide and μ-1,3-carboxylate bridges collaborate to connect Mn(II) ions into formally anionic 2D layers, and the layers are interlinked by positive viologen backbones. The bridging network between Mn(II) ions leads to a spin-canted and long-range ordered antiferromagnetic system with field-induced metamagnetic behaviors. The viologen component imparts photochromic properties to the hybrid material. The reversible color change has been attributed to the formation of viologen radicals via photoinduced electron transfer. The compound represents the first metal-viologen compound that exhibits both long-range magnetic ordering and photochromic properties. Furthermore, the electron transfer character of the viologen ligand allows us to observe photoresponsive magnetic properties. This work demonstrates a new strategy to design molecular photomagnetic materials.

■ ASSOCIATED CONTENT

Ⓢ Supporting Information

The Supporting Information is available free of charge on the ACS Publications website at DOI: 10.1021/acs.inorgchem.5b01888.

Additional plots (PDF)
Crystallographic information for compounds **1** (CIF)

■ AUTHOR INFORMATION

Corresponding Author

*E-mail: eqgao@chem.ecnu.edu.cn.

Notes

The authors declare no competing financial interest.

■ ACKNOWLEDGMENTS

This work is supported by the National Natural Science Foundation of China (NSFC Nos. 21471057 and 21173083) and the Research Fund for the Doctoral Program of Higher Education of China.

■ REFERENCES

(1) Ungur, L.; Lin, S. Y.; Tang, J.; Chibotaru, L. F. *Chem. Soc. Rev.* **2014**, *43*, 6894−6905.

(2) (a) Bianchi, A.; Delgado-Pinar, E.; García-España, E.; Giorgi, C.; Pina, F. *Coord. Chem. Rev.* **2014**, *260*, 156−215. (b) Irie, M.; Fukaminato, T.; Matsuda, K.; Kobatake, S. *Chem. Rev.* **2014**, *114*, 12174−12277.

(3) Ratera, I.; Veciana, J. *Chem. Soc. Rev.* **2012**, *41*, 303−349.

(4) Zhang, T.; Lin, W. *Chem. Soc. Rev.* **2014**, *43*, 5982−5993.

(5) (a) Guldi, D. M.; Rahman, G. M. A.; Sgobba, V.; Ehli, C. *Chem. Soc. Rev.* **2006**, *35*, 471−487. (b) Train, C.; Gruselle, M.; Verdaguer, M. *Chem. Soc. Rev.* **2011**, *40*, 3297−3312. (c) Li, P.-X.; Wang, M.-S.; Cai, L.-Z.; Wang, G.-E.; Guo, G.-C. *J. Mater. Chem. C* **2015**, *3*, 253−256. (d) Liao, J. Z.; Zhang, H. L.; Wang, S. S.; Yong, J. P.; Wu, X. Y.; Yu, R.; Lu, C. Z. *Inorg. Chem.* **2015**, *54*, 4345−4350.

(6) (a) Deng, H.; Doonan, C. J.; Furukawa, H.; Ferreira, R. B.; Towne, J.; Knobler, C. B.; Wang, B.; Yaghi, O. M. *Science* **2010**, *327*, 846−850. (b) Ryder, M.; Tan, J. *Mater. Sci. Technol.* **2014**, *30*, 1598−1612. (c) Wang, M.-S.; Xu, G.; Zhang, Z.-J.; Guo, G.-C. *Chem. Commun.* **2010**, *46*, 361−376. (d) Pardo, R.; Zayat, M.; Levy, D. *Chem. Soc. Rev.* **2011**, *40*, 672−687. (e) Clemente-Leon, M.; Coronado, E.; Marti-Gastaldo, C.; Romero, F. M. *Chem. Soc. Rev.* **2011**, *40*, 473−497.

(7) (a) Sato, O. *Acc. Chem. Res.* **2003**, *36*, 692−700. (b) Ababei, R.; Pichon, C.; Roubeau, O.; Li, Y.-G.; Bréfuel, N.; Buisson, L.; Guionneau, P.; Mathonière, C.; Clérac, R. *J. Am. Chem. Soc.* **2013**, *135*, 14840−14853. (c) Liu, T.; Zheng, H.; Kang, S.; Shiota, Y.; Hayami, S.; Mito, M.; Sato, O.; Yoshizawa, K.; Kanegawa, S.; Duan, C. *Nat. Commun.* **2013**, *4*, 2826.

(8) (a) Alley, K. G.; Poneti, G.; Robinson, P. S.; Nafady, A.; Moubaraki, B.; Aitken, J. B.; Drew, S. C.; Ritchie, C.; Abrahams, B. F.; Hocking, R. K.; Murray, K. S.; Bond, A. M.; Harris, H. H.; Sorace, L.; Boskovic, C. *J. Am. Chem. Soc.* **2013**, *135*, 8304−8323. (b) Sato, O.; Cui, A.; Matsuda, R.; Tao, J.; Hayami, S. *Acc. Chem. Res.* **2007**, *40*, 361−369.

(9) (a) Tao, J.; Wei, R.-J.; Huang, R.-B.; Zheng, L.-S. *Chem. Soc. Rev.* **2012**, *41*, 703−737. (b) Azuma, M.; Chen, W.-t.; Seki, H.; Czapski, M.; Olga, S.; Oka, K.; Mizumaki, M.; Watanuki, T.; Ishimatsu, N.; Kawamura, N.; Ishiwata, S.; Tucker, M. G.; Shimakawa, Y.; Attfield, J. P. *Nat. Commun.* **2011**, *2*, 347. (c) Ohkoshi, S.-i.; Imoto, K.; Tsunobuchi, Y.; Takano, S.; Tokoro, H. *Nat. Chem.* **2011**, *3*, 564−569. (d) Pajerowski, D. M.; Ravel, B.; Li, C. H.; Dumont, M. F.; Talham, D. R. *Chem. Mater.* **2014**, *26*, 2586−2594.

(10) (a) Deska, M.; Kozlowska, J.; Sliwa, W. *ARKIVOC* **2013**, 66−100. (b) Mercier, N. *Eur. J. Inorg. Chem.* **2013**, *2013*, 19−31. (c) Toma, O.; Mercier, N.; Allain, M.; Kassiba, A. A.; Bellat, J. P.; Weber, G.; Bezverkhyy, I. *Inorg. Chem.* **2015**, *54*, 8923−8930. (d) Leblanc, N.; Bi, W.; Mercier, N.; Auban-Senzier, P.; Pasquier, C. *Inorg. Chem.* **2010**, *49*, 5824−5833.

(11) (a) Periyat, P.; Leyland, N.; McCormack, D. E.; Colreavy, J.; Corr, D.; Pillai, S. C. *J. Mater. Chem.* **2010**, *20*, 3650−3655. (b) Moon, H. C.; Lodge, T. P.; Frisbie, C. D. *Chem. Mater.* **2015**, *27*, 1420−1425. (c) Stolar, M.; Borau-Garcia, J.; Toonen, M.; Baumgartner, T. *J. Am. Chem. Soc.* **2015**, *137*, 3366−3371.

(12) (a) Sampanthar, J.; Neoh, K.; Ng, S.; Kang, E.; Tan, K. *Adv. Mater.* **2000**, *12*, 1536−1539. (b) Shi, Z.; Neoh, K. G.; Kang, E. T. *Biomaterials* **2005**, *26*, 501−508.

(13) (a) Trabolsi, A.; Khashab, N.; Fahrenbach, A. C.; Friedman, D. C.; Colvin, M. T.; Cotí, K. K.; Benítez, D.; Tkatchouk, E.; Olsen, J.-C.; Belowich, M. E.; Carmielli, R.; Khatib, H. A.; Goddard, W. A.; Wasielewski, M. R.; Stoddart, J. F. *Nat. Chem.* **2010**, *2*, 42−49. (b) Zhu, L.; Yan, H.; Wang, X. J.; Zhao, Y. *J. Org. Chem.* **2012**, *77*, 10168−10175. (c) Cantekin, S.; Markvoort, A. J.; Elemans, J. A.; Rowan, A. E.; Nolte, R. J. *J. Am. Chem. Soc.* **2015**, *137*, 3915−3923.

(14) (a) Kannappan, R.; Bucher, C.; Saint-Aman, E.; Moutet, J.-C.; Milet, A.; Oltean, M.; Metay, E.; Pellet-Rostaing, S.; Lemaire, M.; Chaix, C. *New J. Chem.* **2010**, *34*, 1373−1386. (b) Kumar, B.; Rao, K. V.; Sampath, S.; George, S. J.; Eswaramoorthy, M. *Angew. Chem.* **2014**, *126*, 13289−13293. (c) Juetten, M. J.; Buck, A. T.; Winter, A. H. *Chem. Commun.* **2015**, *51*, 5516−5519.

(15) (a) Barnes, J. C.; Juricek, M.; Strutt, N. L.; Frasconi, M.; Sampath, S.; Giesener, M. A.; McGrier, P. L.; Bruns, C. J.; Stern, C. L.; Sarjeant, A. A.; Stoddart, J. F. *J. Am. Chem. Soc.* **2013**, *135*, 183−192. (b) Barnes, J. C.; Fahrenbach, A. C.; Cao, D.; Dyar, S. M.; Frasconi, M.; Giesener, M. A.; Benitez, D.; Tkatchouk, E.; Chernyashevskyy, O.; Shin, W. H.; Li, H.; Sampath, S.; Stern, C. L.; Sarjeant, A. A.; Hartlieb, K. J.; Liu, Z.; Carmieli, R.; Botros, Y. Y.; Choi, J. W.; Slawin, A. M. Z.; Ketterson, J. B.; Wasielewski, M. R.; Goddard, W. A., III; Stoddart, J. F. *Science* **2013**, *339*, 429−433. (c) Barnes, J. C.; Fahrenbach, A. C.; Dyar, S. M.; Frasconi, M.; Giesener, M. A.; Zhu, Z.; Liu, Z.; Hartlieb, K. J.; Carmieli, R.; Wasielewski, M. R.; Stoddart, J. F. *Proc. Natl. Acad. Sci. U. S. A.* **2012**, *109*, 11546−11551. (d) Fahrenbach, A. C.; Barnes, J. C.; Lanfranchi, D. A.; Li, H.; Coskun, A.; Gassensmith, J. J.; Liu, Z.; Benitez, D.; Trabolsi, A.; Goddard, W. A.; Elhabiri, M.; Stoddart, J. F. *J. Am. Chem. Soc.* **2012**, *134*, 3061−3072.

(16) (a) Higuchi, M.; Tanaka, D.; Horike, S.; Sakamoto, H.; Nakamura, K.; Takashima, Y.; Hijikata, Y.; Yanai, N.; Kim, J.; Kato, K.; Kubota, Y.; Takata, M.; Kitagawa, S. *J. Am. Chem. Soc.* **2009**, *131*, 10336−10337. (b) Higuchi, M.; Nakamura, K.; Horike, S.; Hijikata, Y.; Yanai, N.; Fukushima, T.; Kim, J.; Kato, K.; Takata, M.; Watanabe, D. *Angew. Chem.* **2012**, *124*, 8494−8497. (c) Lin, J.-B.; Shimizu, G. K. H. *Inorg. Chem. Front.* **2014**, *1*, 302−305. (d) Aulakh, D.; Varghese, J. R.; Wriedt, M. *Inorg. Chem.* **2015**, *54*, 1756−1764. (e) Sun, J.-K.; Yao, Q.-X.; Tian, Y.-Y.; Wu, L.; Zhu, G.-S.; Chen, R.-P.; Zhang, J. *Chem. - Eur. J.* **2012**, *18*, 1924−1931. (f) Sun, J.-K.; Ji, M.; Chen, C.; Wang, W.-G.; Wang, P.; Chen, R.-P.; Zhang, J. *Chem. Commun.* **2013**, *49*, 1624−1626. (g) Jin, X.-H.; Sun, J.-K.; Xu, X.-M.; Li, Z.-H.; Zhang, J. *Chem. Commun.* **2010**, *46*, 4695−4697. (h) Sun, J.-K.; Zhang, J. *Dalton Trans.* **2015**, *44*, 19041−19055.

(17) (a) Tan, Y.; Fu, Z.; Zeng, Y.; Chen, H.; Liao, S.; Zhang, J.; Dai, J. *J. Mater. Chem.* **2012**, *22*, 17452−17455. (b) Sun, J.-K.; Wang, P.; Yao, Q.-X.; Chen, Y.-J.; Li, Z.-H.; Zhang, Y.-F.; Wu, L.-M.; Zhang, J. *J. Mater. Chem.* **2012**, *22*, 12212−12219. (c) Sun, J.-K.; Wang, P.; Chen, C.; Zhou, X.-J.; Wu, L.-M.; Zhang, Y.-F.; Zhang, J. *Dalton Trans.* **2012**, *41*, 13441−13446. (d) Jin, X.-H.; Sun, J.-K.; Xu, X.-M.; Li, Z.-H.; Zhang, J. *Chem. Commun.* **2010**, *46*, 4695−4697.

(18) (a) Sun, J.-K.; Cai, L.-X.; Chen, Y.-J.; Li, Z.-H.; Zhang, J. *Chem. Commun.* **2011**, *47*, 6870−6872. (b) Chen, H.; Li, M.; Zheng, G.; Wang, Y.; Song, Y.; Han, C.; Fu, Z.; Liao, S.; Dai, J. *RSC Adv.* **2014**, *4*, 42983−42990. (c) Chen, H.; Zheng, G.; Li, M.; Wang, Y.; Song, Y.; Han, C.; Dai, J.; Fu, Z. *Chem. Commun.* **2014**, *50*, 13544−13546. (d) Jin, X.-H.; Ren, C.-X.; Sun, J.-K.; Zhou, X.-J.; Cai, L.-X.; Zhang, J. *Chem. Commun.* **2012**, *48*, 10422−10424. (e) Jin, X.-H.; Sun, J.-K.; Cai, L.-X.; Zhang, J. *Chem. Commun.* **2011**, *47*, 2667−2669.

(19) Sun, J.-K.; Chen, C.; Cai, L.-X.; Ren, C.-X.; Tan, B.; Zhang, J. *Chem. Commun.* **2014**, *50*, 15956−15959.

(20) (a) Zhang, H.-X.; Yao, Q.-X.; Jin, X.-H.; Ju, Z.-F.; Zhang, J. *CrystEngComm* **2009**, *11*, 1807−1810. (b) Yao, Q.-X.; Ju, Z.-F.; Jin, X.-H.; Zhang, J. *Inorg. Chem.* **2009**, *48*, 1266−1268. (c) Yao, Q.-X.; Pan, L.; Jin, X.-H.; Li, J.; Ju, Z.-F.; Zhang, J. *Chem. - Eur. J.* **2009**, *15*, 11890−11897.

(21) (a) Wang, Y.-Q.; Sun, W.-W.; Wang, Z.-D.; Jia, Q.-X.; Gao, E.-Q.; Song, Y. *Chem. Commun.* **2011**, *47*, 6386−6388. (b) Wang, Y.-Q.;

Cheng, A.-L.; Liu, P.-P.; Gao, E.-Q. *Chem. Commun.* **2013**, *49*, 6995−6997. (c) Zhang, J. Y.; Wang, K.; Li, X. B.; Gao, E. Q. *Inorg. Chem.* **2014**, *53*, 9306−9314. (d) Wang, Y. Q.; Liu, H. T.; Qi, Y.; Gao, E. Q. *Dalton Trans.* **2014**, *43*, 11819−11825. (e) Wang, Y. Q.; Zhang, X. M.; Li, X. B.; Wang, B. W.; Gao, E. Q. *Inorg. Chem.* **2011**, *50*, 6314−6322.

(22) Kamogawa, H.; Sato, S. *Bull. Chem. Soc. Jpn.* **1991**, *64*, 321−323.

(23) Sheldrick, G. Bruker-AXS: Madison, WI, 2003.

(24) Sheldrick, G. Bruker Analytical X-ray Instruments Inc.: Madison, WI, 1998.

(25) Bongard, D.; Möller, M.; Rao, S. N.; Corr, D.; Walder, L. *Helv. Chim. Acta* **2005**, *88*, 3200−3209.

(26) (a) Kim, Y.; Teshima, K.; Kobayashi, N. *Electrochim. Acta* **2000**, *45*, 1549−1553. (b) Yoshikawa, H.; Nishikiori, S.-I. *Chem. Lett.* **2000**, 142−143.

(27) Xu, G.; Guo, G.-C.; Guo, J.-S.; Guo, S.-P.; Jiang, X.-M.; Yang, C.; Wang, M.-S.; Zhang, Z.-J. *Dalton Trans.* **2010**, *39*, 8688−8692.

(28) (a) Finn, P.; Jolly, W. L. *Inorg. Chem.* **1972**, *11*, 1434−1435. (b) Zhang, J.; Matsushita, M. M.; Kong, X. X.; Abe, J.; Iyoda, T. *J. Am. Chem. Soc.* **2001**, *123*, 12105−12106.

(29) (a) Ribas, J.; Escuer, A.; Monfort, M.; Vicente, R.; Cortes, R.; Lezama, L.; Rojo, T. *Coord. Chem. Rev.* **1999**, *193−195*, 1027−1068. (b) Wang, X. Y.; Wang, Z. M.; Gao, S. *Chem. Commun.* **2008**, *3*, 281−294.

(30) (a) Wang, Y.-Q.; Yue, Q.; Qi, Y.; Wang, K.; Sun, Q.; Gao, E.-Q. *Inorg. Chem.* **2013**, *52*, 4259−4268. (b) Zhuang, G. M.; Li, X. B.; Wen, Y. Q.; Tian, C. Y.; Gao, E. Q. *Eur. J. Inorg. Chem.* **2014**, *2014*, 3488−3498. (c) He, Z.; Wang, Z.-M.; Gao, S.; Yan, C.-H. *Inorg. Chem.* **2006**, *45*, 6694−6705. (d) Yang, Q.; Zhao, J.-P.; Hu, B.-W.; Zhang, X.-F.; Bu, X.-H. *Inorg. Chem.* **2010**, *49*, 3746−3751. (e) Wang, Y. Q.; Sun, Q.; Yue, Q.; Cheng, A. L.; Song, Y.; Gao, E. Q. *Dalton Trans.* **2011**, *40*, 10966−10974. (f) Zhang, X. M.; Wang, Y. Q.; Song, Y.; Gao, E. Q. *Inorg. Chem.* **2011**, *50*, 7284−7294.

(31) Ruiz, E.; Cano, J.; Alvarez, S.; Alemany, P. *J. Am. Chem. Soc.* **1998**, *120*, 11122−11129.

(32) (a) Gao, E.-Q.; Wang, Z.-M.; Yan, C.-H. *Chem. Commun.* **2003**, *14*, 1748−1749. (b) Gao, E.-Q.; Cheng, A.-L.; Xu, Y.-X.; He, M.-Y.; Yan, C.-H. *Inorg. Chem.* **2005**, *44*, 8822−8835.

(33) Kahn, O. *Molecular Magnetism*; VCH: New York, 1993.

(34) Bellitto, C.; Federici, F.; Colapietro, M.; Portalone, G.; Caschera, D. *Inorg. Chem.* **2002**, *41*, 709−714.